Mathematical Modeling of Optical-Fiber Refractometric Device

VLADIMIR SVIRID, SERGEI KHOTIAINTSEV
Department of Electrical Engineering, Faculty of Engineering
National Autonomous University of Mexico
Ciudad Universitaria, c. p. 04510, Mexico, D. F.
MEXICO

PIETER L. SWART
Faculty of Engineering
Rand Afrikaans University
Auckland Park 2006, Johannesburg, PO Box 524
REPUBLIC OF SOUTH AFRICA

Abstract: - We present a ray-tracing application in the modeling of an optical detection element employed as a sensor of refractive index of surrounding fluids or gases. The detection element is a solid glass microstructure having a surface of the second order. We exploit the sensitivity of internal reflection of light on the element's surface to the refractive index of the surrounding medium, operation near the critical angle of incidence, several internal reflections in series, and the focusing properties of the concave surface. We present the techniques employed in the numerical modeling of the detection element. These techniques permitted to reduce significantly the computing time and memory size necessary for accessing the operational characteristics of the detection element.

Key-Words: - Mathematical modeling, optical design software, numerical ray tracing, optical instrumentation, refractive index measurement, optoelectronic sensors.

1 Introduction

Numerical ray tracing has many useful applications in the analysis of optical structures. Some work has been made in the field of optical fiber sensors of refractometric type [1]-[3]. Recently, we have reported a novel optical-fiber refractometric detection element [1] that employs the liquid-dependent total internal reflection on the element's hemispherical surface. This transducer showed characteristics suitable for many important applications.

This paper presents a mathematical model and three calculation algorithms used in the analysis of optical detection elements having the surfaces of the first and second order. We accessed the element's sensitivity to the refractive index of the surrounding media as a function of device geometrical parameters and material constants.

The generic structure of the device that we treat here consists of three principal parts: a transmitting multimode optical fiber, a solid glass element with the first-order or second-order surface, and a receiving multimode optical fiber (see Fig 1). The optical fibers connect the glass element with the remote light source (typically, light-emitting diode) and an optical receiver (light intensity meter) not shown in Fig 1. The two optical fibers are coupled via one or several sequential total internal reflections on the element's surface. The amount of coupling depends on the refractive index of surrounding media as well as on the geometrical parameters and material constants of the device.

The mathematical modeling of this device presents many difficulties because the device employs non-coherent optical beams of relatively large divergence and cross section. In addition, the device lacks the axis of symmetry. The principal difficulty, however, is related to the high sensitivity of the device operational characteristics (such as the sensitivity to refractive index of surrounding medium, input span, non-linearity, etc.) even to small variations of device parameters. The high sensitivity results from the device operation under the angle of incidence of the

input light on the element's surface that is very close to the critical one. Such regime secures an enhanced sensitivity of the device to the refractive index of the surrounding medium [2]. But, to access the device characteristics through numerical ray tracing with sufficient accuracy, one should use a very large number of rays (In the present work, we employed 100,000 rays for the modeling of optical beam). The large number of rays, in the general case, requires a large computer memory and large computing time. It will thus be of interest to study the mathematical modeling of the present device. In particular, to study how the necessary computing time and memory size can be reduced in accessing the operational characteristics of the device.

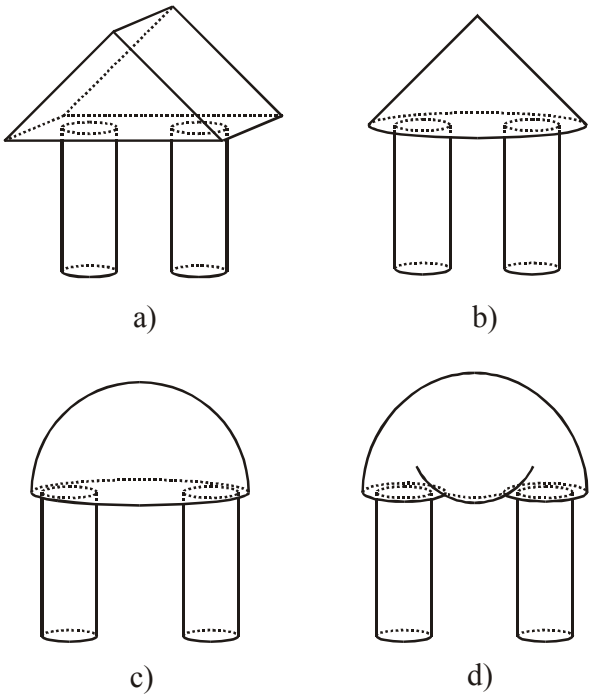

Fig 1. Examples of refractometric devices consisting of the transmitting and receiving optical fibers integrated with the detection element. The element's refractometric surface has the form of the prism (a), cone (b), hemisphere (c), and the second-order surface (d).

2 Initial Assumptions

We now consider the detection element of the transparent dielectric material of the refractive index n_e. Two multimode optical fibers may have the identical or different core diameter d and numerical aperture NA. Both optical fibers are at right angle to the element flat surface and are placed symmetrically with respect to the common system axis. For the analysis of the refractometric properties of the detection element, we introduce the relative transmission function

$$T^*(n) = \frac{I_2(n)/I_1}{I_{2air}/I_1} = \frac{I_2(n)}{I_{2air}}, \qquad (1)$$

I_1 is the intensity of the input light (i.e. the light launched into the detection element from the transmitting fiber), $I_2(n)$ is the intensity of the element output light (i.e. the light accepted by the receiving fiber core; this quantity is a function of the refractive index of the surrounding medium n), and I_{2air} is the intensity of the element output light when the surrounding medium is air (n=1).

3 Mathematical Modeling of Device

In order to analyze theoretically the optical properties of the present device, we developed a mathematical model suitable for the numerical ray tracing. The need in special model differing from the majority of existing models [3] is determined by the fact that the present device is an essentially three-dimensional structure that has no axis of symmetry. In addition, because of the large beam divergence typical in optical fiber devices, no paraxial approximation is applicable in light propagation analysis. Also, the complex device form determines the need in a special model. The above mentioned properties require some special features not available in already existing optical ray tracing software.

In this work, we employed the optical transmission function of the device as the basic element of the device mathematical model. For the intensity type optical sensors, the output quantity is usually the electrical current of the photo detector. Thereby, device transmission function was defined as a function of the photo receiver current I_r versus the measurand (the refractive index of the surrounding medium n). The photo receiver current can be expressed in terms of the device parameters

$$I_r(n) = P_s \; T_0 \; T^*(n) \; S_r, \qquad (2)$$

P_s is the optical source power, $T^*(n)$ is the relative transmission function of the device, S_r is the receiver sensitivity, T_0 is the intrinsic loss factor (The optical attenuation in the device when the detection element is in the air).

In the case when the photo receiver sensitivity S_r does not depend on the input light intensity and the

intrinsic loss factor T_0 is constant, then the photo receiver current I_r is a measure of the refractive index of the surrounding medium n.

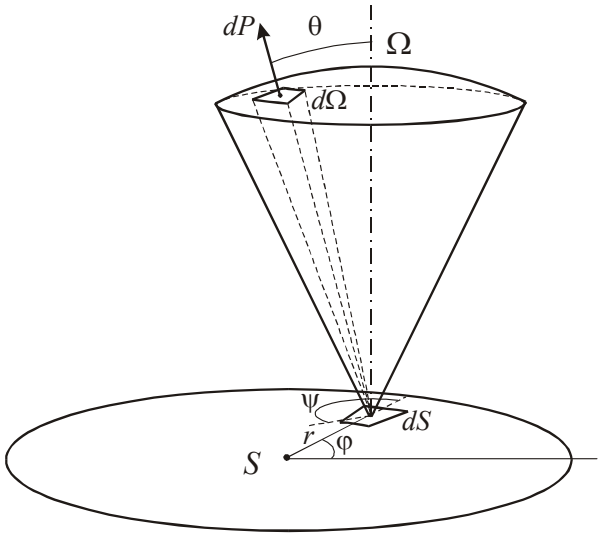

Fig 2. The system of coordinates used in the definition of the radiation flux element dP. S is the total area of the emitting surface (transmitting fiber core); dS is the emitting surface element; Ω is the solid angle corresponding to the angular aperture of the optical fiber; $d\Omega$ is the solid angle element; r, φ are the polar coordinates of the emitting surface element with reference to the fiber center; θ, ψ are the spherical polar coordinates of the solid angle element axis with reference to the fiber axis.

For the calculation of the device transmission function it is expedient to employ the geometrical optics methods. Let us find the element of the total radiation flux dP that is emitted by the surface element dS within the solid angle element $d\Omega$. In the general case shown in Fig 2

$$dP = J(r,\varphi,\theta,\psi)\ dS\ d\Omega\ = \\ = J(r,\varphi,\theta,\psi)\ r\ dr\ d\varphi\ sin\theta\ d\theta\ d\psi, \tag{3}$$

$J(r, \varphi, \theta, \psi)$ is the power distribution over the emitting surface and over the ray exit directions; r, φ are the polar coordinates of the emitting surface element with reference to the fiber center; θ, ψ are the spherical polar coordinates of the solid angle element axis with reference to the fiber axis.

We accounted for the radiation flux $P_2(n)$ in the receiving optical fiber by integration of the expression describing an evolution of the elementary ray that propagates from the transmitting fiber to the receiving one. At this derivation, we accounted for the initial value of the flux element dP, flux attenuation caused by the partial reflection at the detection element surface, and the loss of the rays, which do not arrive at the receiving fiber aperture:

$$P_2(n) = \iint_A \iint_\Omega J(r,\varphi,\theta,\psi)\ \ R(n,\alpha(r,\varphi,\theta,\psi,F)) \\ M(r,\varphi,\theta,\psi,F,K)\ \ r\ dr\ d\varphi\ \ \text{sen}\,\theta\ d\theta\ d\psi, \tag{4}$$

R is the function describing ray attenuation caused by the reflection at the detection element surface; α is angle of incidence of the elementary ray on the element's surface; M is the function of ray arrival at the receiving fiber aperture; F is the function describing the shape of the detection element surface, K is the function describing the size and coordinates of the receiving fiber aperture.

In the present work, we assumed a monochromatic, non-polarized, and non-coherent light. The reflection coefficient R was derived in accordance with the well-known Fresnel formula for the non-polarized light

$$R = \frac{1}{2}\left[\frac{(n/n_e)^2\cos\alpha - \sqrt{(n/n_e)^2 - sin^2\alpha}}{(n/n_e)^2\cos\alpha + \sqrt{(n/n_e)^2 - sin^2\alpha}}\right]^2 + \\ + \frac{1}{2}\left[\frac{\cos\alpha - \sqrt{(n/n_e)^2 - sin^2\alpha}}{\cos\alpha + \sqrt{(n/n_e)^2 - sin^2\alpha}}\right]^2, \tag{5}$$

In the modeling, we represented the surface of the detection element by the corresponding analytical equation. In the case of the elements b, c, d shown in Fig 1, the surface was described by the second-order equation

$$a_{11}x^2 + a_{22}y^2 + a_{33}z^2 + 2a_{12}xy + 2a_{13}xz + \\ + a_{23}yz + a_{14}x + a_{24}y + a_{34}z + a_{44} = 0, \tag{6}$$

a_{11} - a_{44} are the coefficients describing the second-order surface; x, y, z are the Cartesian coordinates of the points of the surface.

The mathematical model accounted for the optical fiber core diameter, optical beam divergence, position of the optical fibers with respect to the system axis, and light intensity distribution across the beam.

4 Computational Algorithms

The basic version of the computer algorithm developed for the calculation of the relative transmission function $T^*(n)$ in accordance with the model (1) - (6) is shown in Fig 3. We employed a number of the elementary rays L=100,000 in the modeling of the beam. The ray initial coordinates r and φ and the angles to the fiber axis θ and ψ were assigned at random by employing the Monte-Carlo method.

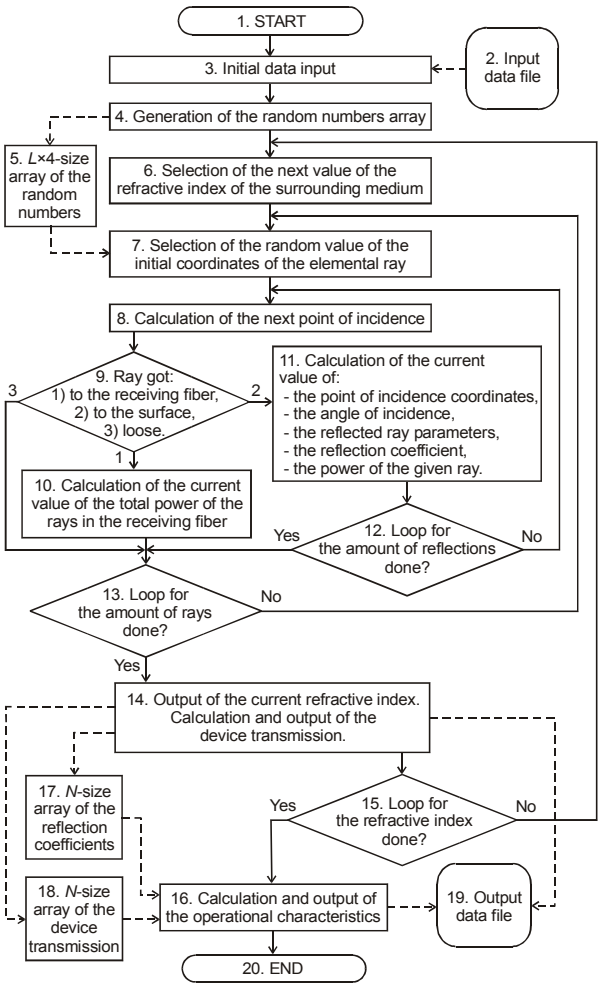

Fig 3. The basic version of the computer algorithm for the calculation of the transmission characteristic of the refractometric device.

The algorithm accounted for serial internal reflections from the element's surface of the number

$$M \le 100.$$

The Fresnel reflection coefficient was calculated at each reflection point and the resulting optical power was determined for each ray. The element's transmission T was found by integrating the contributions of all the rays, which arrived at the receiving fiber core within the limits of its linear and angular aperture.

This algorithm permitted to access the element's transmission with sufficient accuracy and detail but was rather slow because the numerical ray tracing was repeated for L rays and for M serial internal reflections from the element's surface under one particular refractive index of the surrounding media. Then the calculations were repeated for the following refractive index and in this way the transmission function was obtained. In order

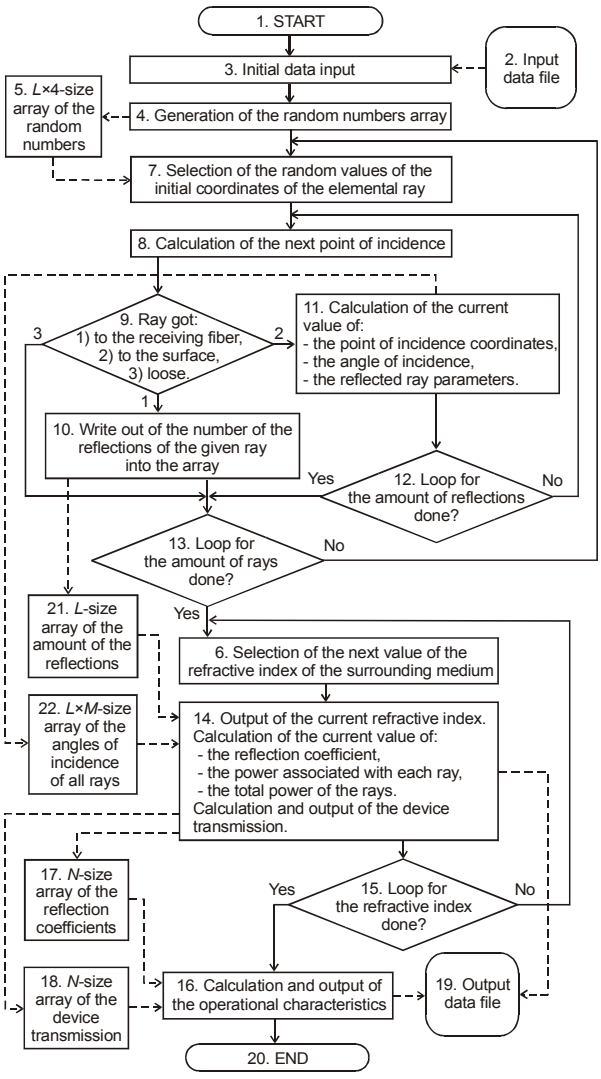

Fig 4. The second version of the algorithm that requires less computer time but larger memory size.

to reduce the computing time necessary for the calculation of the transmission function of the refractometric device we modified the initial algorithm. In the modified version shown in Fig 4, the tracing of each ray is performed only once and the coordinates of serial reflection points on the refractometric surface are found. The angle of incidence is calculated in each of these points and written out into the corresponding $L \times M$ size array. The loop for the refractive index is done and Fresnel reflection coefficient is calculated for all reflection points. Then the total optical power reaching the receiving fiber aperture is calculated. This algorithm saves the computing time but requires a sufficiently large memory to store very large $L \times M$ array.

Substantial reduction of memory requirements was achieved in the next 3rd version of the algorithm shown in Fig 5. According to this algorithm, the angles of incidence of a given ray in serial reflection points on the refractometric surface are written out into the corresponding M size array. Then the loop for the refractive index is done N times and the total power of the given ray is written out into the N size array. During the subsequent loops for the rays and successive refractive indices the current total power of the rays is accumulated in the same N size array. The arrays N and M are relatively small. This presents an important advantage of the present algorithm in comparison to the previous one.

5 Simulation Results

The tests of the developed mathematical model and all three computational algorithms were performed for the detection element with hemispherical surface because of its relatively simple geometrical and optical properties. The parameters were: the dimensionless fiber distance from the element axis l, the dimensionless fiber core diameter d, the refractive index of the element material n_e, and the fiber numerical aperture in the air NA. (In the ray tracing, we employed the beam divergence in the fiber instead of the NA.) The transmission T was calculated for various n and the transmission function $T(n)$ determined.

The experiment showed that the required computing time was less by a factor of 50 for the second version of the algorithm, in comparison to the basic one. However, the required memory size in the second version of the algorithm was larger by a factor of 200, in comparison to the basic one.

The third version of the algorithm required a moderate memory size of roughly the same order as in the case of the basic algorithm. However, the third version worked as fast as the second one. That is, the reduction in the computing time was by a factor of 50 in comparison to the basic version of the algorithm. While the necessary memory size was almost the same as in the case of the basic version of the computational algorithm.

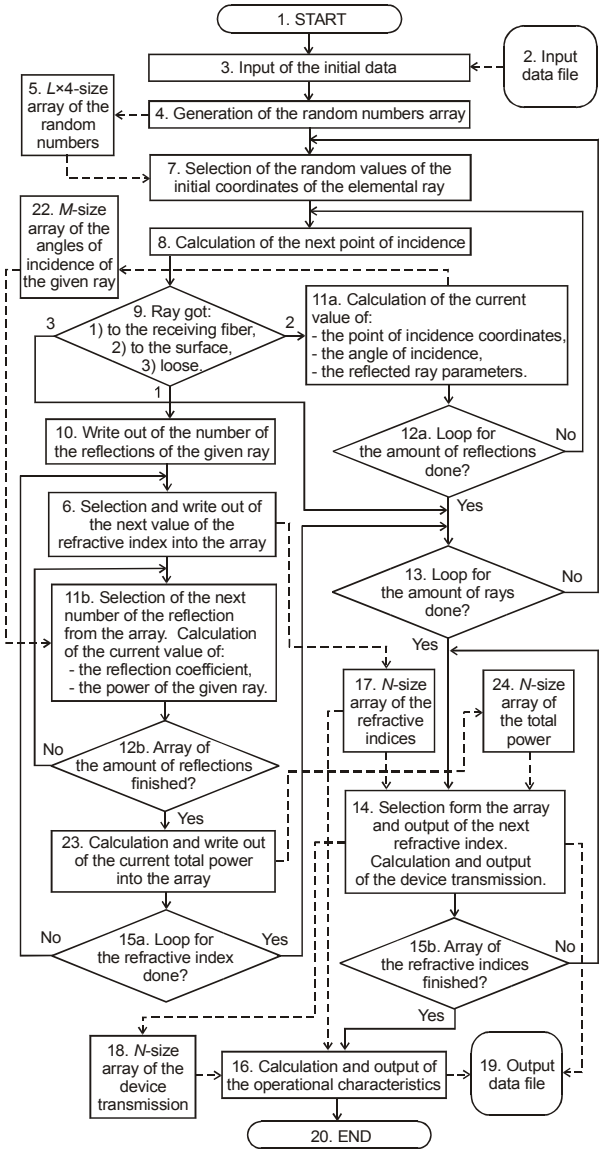

Fig 5. The 3rd version of the computational algorithm that is fast and requires a relatively small memory size for the computation of the transmission function of the refractometric element.

The examples of the calculated relative transmission function $T^*(n)$ are shown in Fig 6 for three different combinations of the device parameters. Curve 1 corresponds to a small angle of incidence of the rays on the refractometric surface and two serial reflections from the surface. Curve 3 corresponds to a large angle of incidence and four serial reflections from the surface. Curve 2 corresponds to a large core diameter and relatively small angular aperture of the optical fibers. In this case, the different groups of rays of the optical beam contribute to the element's transmission in different manner. This results in the complex behavior of curve 2.

One can see from Fig 6 that the relative transmission function exhibits strong dependence on even small variations of the device parameters. At the same time, this permits to modify the form of the relative transmission function from virtually linear (curve 1 and 3) to the essentially non-linear one (curve 2). Also, to change the device input range and sensitivity to the refractive index of surrounding medium. These properties make the transducer attractive for diverse applications.

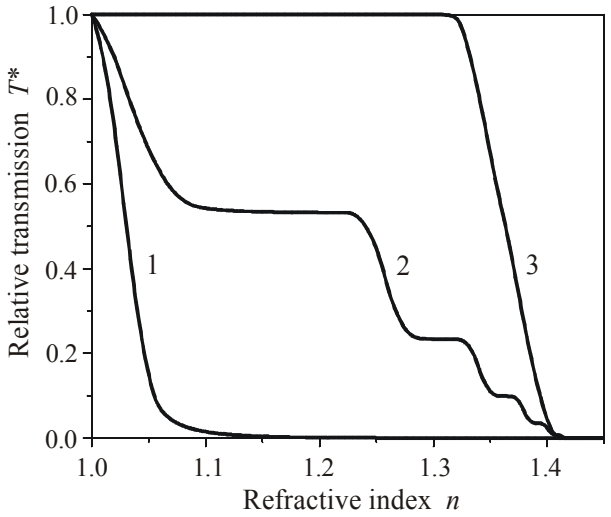

Fig 6. Device relative transmission T* vs. the refractive index of the surrounding medium *n* obtained under different device parameter combinations.

6 Conclusions

We developed the mathematical model and the corresponding computational algorithm that permits to access the refractometric properties of the detection elements of complex form with accuracy and detail sufficient for their analysis and optimization. The developed algorithm is efficient both in terms of computer time and memory size necessary for the calculations.

This permits, in particular, to employ the present algorithm in the analysis of the optical elements having the surfaces of the 3rd and higher orders.

This work was supported by the National Science and Research Council of Mexico (CONACyT) under the Research Project 35001-A. This work was partially supported also by the National Autonomous University of Mexico under the Research Project PAPIIT / DGPA IN113799, and the Centre of Optical Communications, Rand Afrikaans University, Republic of South Africa.

References:

[1] S. Khotiaintsev, V. Svirid, and P. L. Swart, "Novel fiber-optical refractometric sensor employing hemispherically-shaped detection element." / In the book: *Advances in Systems Science: Measurement, Circuits and Control. Electrical and Computer Engineering Series,* WSES Press, 2001, pp. 595-599.

[2] V. Svirid and S. Khotiaintsev, "Primary transducers of discrete fiber-optic level gauges," *Measurement Techniques*, Vol.33, No.7, 1990, pp. 679-682.

[3] V. De Leon and S. Khotiaintsev, "Microoptical paraboloidal-shaped sensing elements for refractometric applications," *Instrumentation and Development,* Vol.4, No.1, 1999, pp. 31-39.

[4] V. Svirid, V. De Leon, and S. Khotiaintsev, "A prototype fiber-optic discrete level-sensor for liquid propane-butane," *IEICE Transactions on Electronics*, Vol.E83-C, No.3, 2000, pp. 303-309.